SERI/TP-252-2482
UC Category: 62
DE85000503

Temperature and Heat Flux Distribution in a Natural Convection Enclosure Flow

Mark S. Bohn
Ren Anderson

September 1984

Prepared for the Passive and Hybrid
Solar Energy Update
Washington, DC
5-7 September 1984

Prepared under Task No. 3736.10
FTP No. 468

Solar Energy Research Institute
A Division of Midwest Research Institute

1617 Cole Boulevard
Golden, Colorado 80401

Prepared for the
U.S. Department of Energy
Contract No. DE-AC02-83CH10093

PROJECT SUMMARY

Project Title:

Heat Transfer Research

Performing Institution:

Solar Energy Research Institute
1617 Cole Boulevard
Golden, CO 80401

Project Manager:

Mark Bohn (303)231-1755

Project Objectives:

Of the important mechanisms which transfer heat in building, convection is the most complex and least understood. In the past, heat transfer research has not focused on problems with sufficiently complex boundary conditions, nor at large enough physical length scales to provide information which is clearly applicable to building heat transfer. The objective of this project is to improve our understanding of how heat and air are transported in a passively heated or cooled building. This will lead to design tools for predicting heat and air flow in buildings, and will also lead to improved performance of passively heated or cooled buildings.

Project Status:

The research effort initially focused on investigations of natural convection in relatively simple, three-dimensional enclosures in which the important heat transfer mechanisms and regimes were identified. Heat transfer correlations were developed for heated or cooled vertical surfaces and also for horizontal surfaces in enclosures. Identification of the heat transfer mechanism for vertical surfaces has led to investigations of methods for increasing natural convection heat transfer from vertical surfaces--especially important for utilization of advanced storage materials. Further work determined how the temperature distribution in the case of an enclosure, i.e., room air temperature distribution, is affected by complex heating or cooling boundary conditions.

Plans and Objectives for FY 1984:

In FY 1984 two experimental apparatuses are being fabricated to allow (1) a detailed investigation of natural convection heat transfer enhancement and (2) a study of natural convection in enclosures in the turbulent regime. In the first, a Mach-Zehnder interferometer will allow detailed monitoring of the boundary layer progressing up a heated wall in an air-filled enclosure. Several types of boundary layer trips will be placed on the wall and the effect on the boundary layer and local heat transfer will be observed. In the second experiment, a large (0.6 m cube) water filled enclosure will allow us to achieve fully turbulent boundary layers and to determine heat transfer and core temperature under conditions which model large interior spaces.

Major Publications Related to Project:

"Experimental Study of Three-Dimensional Natural Convection at High-Rayleigh Number," J. Heat Transfer, Vol. 106, pp. 339-345, May 1984.

"Influence of Prandtl Number on Natural Convection Heat Transfer Correlations," SERI/TR-252-2007, July 1984.

"Temperature and Heat Flux Distribution in a Natural Convection Enclosure Flow," submitted to J. Heat Transfer, July 1984.

"Heat Transfer Enhancement in a Natural Convection Enclosure Flow," SERI/TR-252-100, September 1984. Also accepted for presentation at the ASME Winter Annual Meeting, December 1984. Submitted for publication, J. Heat Transfer.

"Natural Convection Heat Transfer in Passive Solar Buildings," accepted for presentation at the 9th National Passive Solar Conference, September 1984.

Contract Number:

DE-AC02-93CH10093

Funding Source:

U.S. Department of Energy

FY 1984 Funding:

$320K

TEMPERATURE AND HEAT FLUX DISTRIBUTION IN A NATURAL CONVECTION ENCLOSURE FLOW

Mark S. Bohn
Ren Anderson

Solar Energy Research Institute
Golden, Colorado 80401

ABSTRACT

This paper presents detailed core temperature distribution measurements and detailed wall heat flux distribution measurements in a three-dimensional enclosure which models a building interior. The objective of this work is to determine if the three-dimensionality of building interiors precludes the usage of available two-dimensional data and correlations for predicting building heat transfer via natural convection.

NOMENCLATURE

g	acceleration of gravity, m/s^2
H	test cell height, m
k	thermal conductivity, W/m^oC
L	test cell length, m
Nu_x	local Nusselt number
$\overline{Nu}$	average Nusselt number
N_{hw}	number of heated walls
Pr	Prandtl number
q	heat flux, W/m^2
Ra_x	local Raleigh number, Eq. (10)
Ra_o	overall Raleigh number, Eq. (2)
T_h	temperature of heated wall, ^oC
T_c	temperature of cooled wall, ^oC
T	temperature, ^oC
T_b	bulk temperature, Eq. (6), ^oC
T_{fm}	mean temperature with heated boundary layer, Eq. (11), ^oC
W	test cell width, m
x	distance from test cell floor, m
y	distance from heated wall, m
z	distance from test cell center plane, m

Greek

β	coefficient of thermal expansion
θ	dimensionless temperature, Eq. (3)
θ_b	average value of θ in the test cell
ν	kinematic viscosity, m^2/s

INTRODUCTION

A vast majority of the extensive literature in natural convection in enclosures has been concerned with two-dimensional geometries. That is, an enclosure consisting of two parallel vertical surfaces held at different temperatures and, with adiabatic or conducting top and bottom. These studies treat an important class of problems with many practical applications. However, by neglecting the third dimension, complexities present in many real problems are also neglected. Of interest in three-dimensional enclosure is heat transfer between parallel as well as perpendicular vertical walls and how the three-dimensional boundary conditions affect the fluid core.

In a recent experimental effort, Bohn et al [1], the first problem was treated in detail: heat transfer between parallel and perpendicular vertical walls. Several important features of three-dimensional natural convection enclosure flows were discussed. The testing in [1] was carried out in a water-filled cubical enclosure with an adiabatic top and bottom and isothermal sides at Rayleigh numbers, $\sim 10^{10}$. The high Rayleigh numbers are of interest in the study of building heat transfer as well as other practical applications. Several configurations of side wall heating and cooling were tested. It was determined that by judicious choice of a reference temperature, the average Nusselt number correlation equation was only weakly configuration dependent. The correct reference temperature was a bulk temperature defined as the average of the four isothermal wall temperatures. By basing the average Nusselt number on the difference between the wall and bulk temperature, correlation equations for all configurations could be collapsed to a single correlation equation

$$\overline{Nu} = 0.620\, Ra_o^{0.250} \quad (1)$$

in the Rayleigh number range $0.3 \times 10^{10} < Ra_o < 6.0 \times 10^{10}$.

Flow visualization studies indicated that the bulk of the test cell fluid was essentially stagnant, the only substantial motion was that in the boundary layers on the vertical surfaces.

The work presented in this paper extends that in [1] to include the effect of three-dimensional boundary conditions on core temperature profiles and on local heat transfer.

EXPERIMENTAL APPARATUS

The experimental apparatus was described in detail in [1] and consists of a cubical enclosure with interior dimension 30.5 cm, Figure 1. The enclosure is filled with water to achieve Rayleigh numbers $\sim 10^{10}$. The boundary conditions include an adiabatic top and bottom and four isothermal vertical walls. In this work two configurations were tested: one heated wall with three cooled walls and two contiguous heated walls with two contiguous cooled walls.

Three of the vertical walls are cooled or heated by flowing water through heat exchanger channels milled into plates that bolt to the outside of the walls. The remaining vertical wall is electrically heated. Sixteen equal area (58.1 cm^2 each) independent heaters are attached to the outside surface of the electrically heated wall. These heaters are controlled by a microcomputer that can provide an isothermal or constant flux boundary condition on that wall as required. In addition, the microcomputer records the power dissipation for each heater, thereby providing information on local heat transfer from that wall. One thermocouple (copper-constantan) senses the temperature of the center of the zone defined by each heater. The thermocouples were located 1 mm from the inner surface of the wall. In the isothermal mode of operation, the computer senses the temperature of the zone, and if it is below the set point, more power is applied to that zone. A proportional-integral control algorithm is used to determine how long each heater should be left on during each cycle of operation, ~10 s. In the second configuration tested (two contiguous heated walls and two continguous cooled walls) the second heated wall was heated with hot water pumped through the heat exchanger channels milled into the external plates.

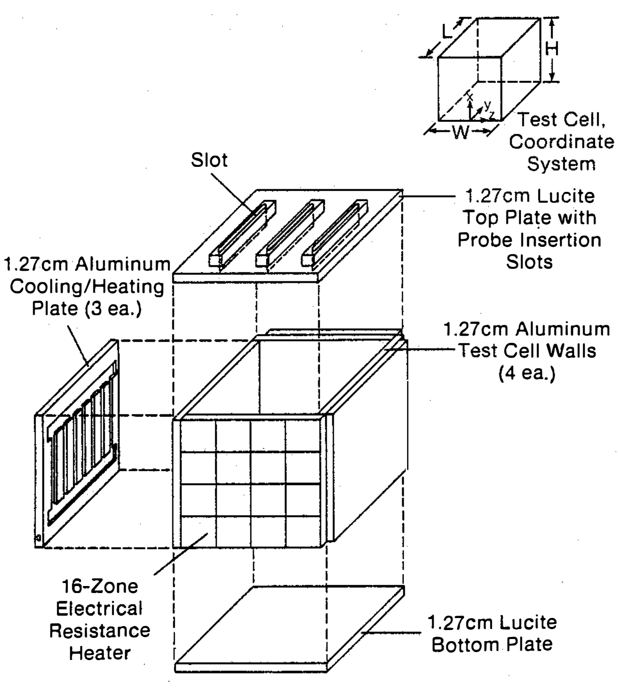

Figure 1. Schematic of Cubical Test Cell

Given the temperature of the heated plates T_h and the temperature of the cooled plates T_c the Rayleigh number is defined by

$$Ra_0 = \frac{g\beta(T_h - T_c)H^3}{\nu^2} Pr \qquad (2)$$

The dimensionless local heat transfer coefficient Nu_x is based on the local heat flux q and the difference in temperature between the wall and the bulk fluid see equation (5). Local heat flux q was determined from local temperature gradient measurements near the heated wall.

Core fluid temperature profiles were measured with a rake consisting of seven, 0.08 mm copper-constantan thermocouples. The rake was inserted vertically through one of three slots 6.4 mm wide cut in the top of the enclosure (see Figure 1). Each slot was perpendicular to the electrically heated wall, and the three slot locations were on the centerline midway between the two parallel cooled walls and 7.62, and 12.70 cm from the center-line. To minimize flow disturbances at the top boundary, lucite inserts were placed in the unused slots. These fit flush in the slot and gave a smooth surface at the water interface. The thermocouples in the rake were located at 0.010, 0.164, 0.331, 0.497, 0.664, 0.831, and 0.997 cell heights (H) from the bottom of the test cell. A traversing mechanism allowed the rake to be moved in the direction y normal to the heated wall with a resolution of 0.025 mm. The temperature measurement from each thermocouple was made dimensionless with the overall temperature difference between the hot and cold walls.

$$\theta = \frac{T - T_c}{T_h - T_c} , \qquad (3)$$

By linear interpolation, the height x from the bottom where θ took values of 0.1, 0.2, ...0.9 was calculated. Connecting points of equal θ for different rake locations y produces contours of constant θ in the test cell, Figure 3.

Since the traversing mechanism did not allow location of the rake closer than 25.4 mm from any vertical surface, an additional probe was used to measure temperature profiles in the boundary layer on the vertical heated wall of the enclosure. This single junction probe (also 0.08 mm, copper-constantan) inserted into the test cell through an angled sheath, allowed the probe to be placed in contact with the heated surface and traversed out from the surface. In this way, high spatial resolution was achieved as needed in the thermal boundary layer. The ability to relocate the single probe at the exact location where a junction of the rake probe had been located was indicated in an error in θ of less than 0.01.

The local heat flux on the heated wall was calculated by determining the temperature gradient at the wall from the measured boundary layer temperature profile. A least-squares fit of the five temperature measurements near the wall (at distance y = 0, 0.0508, 0.102, 0.152, and 0.203 mm) gives dθ/dy at the wall. The local heat flux is then

$$q(x) = \frac{d\theta}{dy}(T_h - T_c)k \quad . \tag{4}$$

The correlation coefficient for this least squares procedure was typically 0.99^+. Equation (4) can be cast in dimensionless form to produce the local Nusselt number

$$Nu_x = \frac{q(x)}{(T_h - T_c)}\frac{H}{k} = \frac{d\theta}{dy}H \quad . \tag{5}$$

In [1], the bulk fluid temperature was defined as the area-weighted average of the four isothermal wall temperatures:

$$T_b = \frac{1}{4}[N_{hw}T_h + (4 - N_{hw})\,T_c] \quad , \tag{6}$$

where N_{hw} is the number of heated walls in the experiment. This definition was based on a heuristic argument rather than actual core fluid temperature measurements. As mentioned previously, it was shown in [1] that this choice of bulk fluid temperature collapsed data for all heating/cooling configurations onto one curve supporting our argument that the wall-to-bulk temperature difference is the correct temperature difference to use in scaling heat transfer results in enclosures with complex thermal boundary conditions. In this paper we demonstrate that the bulk temperature defined by equation (6) is a good estimate of the actual average core temperature.

Temperature measurement errors are < ±0.25°C, which produces an error in θ of approximately ±0.01 for $T_h - T_c \approx 28°C$ for the core temperature profile. This error resulted primarily because two data acquisition systems were used to facilitate data plotting during the measurement of core temperatures and there was some discrepancy in the temperature measured by each system. For the boundary layer measurements only one of the data acquisitions systems was used, and the error in θ is ±0.005 or less. Note that the finite size of the probe junction produces some loss in spatial resolution. A typical thermal boundary layer thickness was 2.5 mm, and the probe junction was approximately 0.48 mm or 19% of the boundary layer thickness. It is interesting to note that producing the thermocouple junction (by spot welding for this study) produces a junction six times the diameter of the individual wires. The effect of finite probe size is two-fold. First, the boundary layer profiles are shifted away from the wall because the junction cannot be placed exactly at the wall surface. Second, the probe will tend to integrate the temperature distribution over the physical extent of the junction. The first effect may be seen in the dimensionless boundary layer temperature profiles which appear to be shifted approximately one junction diameter from the heated wall. These boundary layer profiles were not corrected for this spatial shift. The second effect should have minimal effect since the junction is integrating over a linear portion of the temperature profile and the measured temperature should correspond closely to that at the center of the junction.

To minimize errors caused by flow interference and to minimize probe conduction errors, the probe lead wires were encased in a glass capillary tube, see Figure 2. Assuming the lead wires are at the core fluid temperature where the glass tube joins the steel sheath, the error in indicated temperature caused by conduction along the wires is less than -0.1°C, or an error in θ of -0.004. Results were not corrected for this error.

RESULTS AND DISCUSSION

A core temperature distribution is presented in Figure 3. The distribution represents measurements in plane defined by z = 0, see Figure 1. Temperature distributions were also measured in planes defined by z/W = 0.25 and z/W = 0.417 but are not

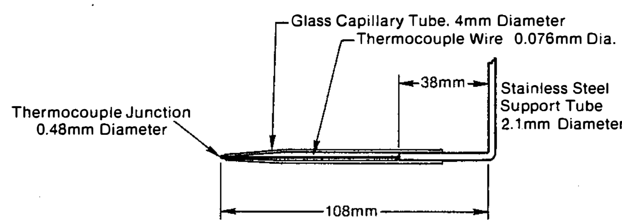

Figure 2. Probe for Boundary Layer Temperature Measurements

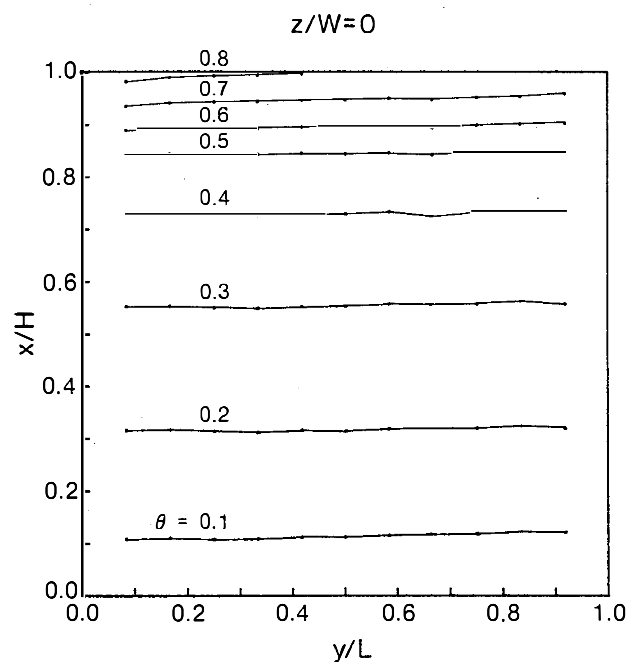

Figure 3. Temperature Distribution in the Core, z = 0, $Ra_0 = 1 \times 10^{10}$

presented here because they are nearly identical to the distribution in Figure 3. Isotherms representing θ = 0.1, 0.2, 0.3, 0.4, 0.5, 0.6, 0.7, and 0.8 are shown. During these tests, the heated wall was held at 40°C and the three cooled walls at approximately 12°C, giving $Ra_o \cong 1.0 \times 10^{10}$, with a measurement error of $-0, +0.03 \times 10^{10}$.

That these isotherm plots were found to be independent of z demonstrates that the core is essentially stratified and the temperature profiles in the core are essentially one-dimensional in nature. That is, the core temperature may be fully characterized by a vertical temperature gradient alone. For the plane z = 0 the centerline temperature profile (along the vertical line at y = L/2) and the centerline distribution for the geometry with two heated walls is shown in Figure 4 along with the centerline temperature distribution in a two-dimensional enclosure, Cowan (2) and Ozoe et al. (3). The three-dimensional profile from the present work for a single heated wall appears to be shifted to low values of θ relative to the two-dimensional profiles, while the profile for two heated and two cooled walls compares favorably with the profiles shown in Figure 4 for the two-dimensional enclosures. In the present experiment, the three cooled walls and one heated wall forces the bulk fluid temperature lower than geometries with equal heated and cooled areas. This is consistent with the heuristic argument used in [1] to show that the appropriate bulk fluid temperature should be that given by equation (6).

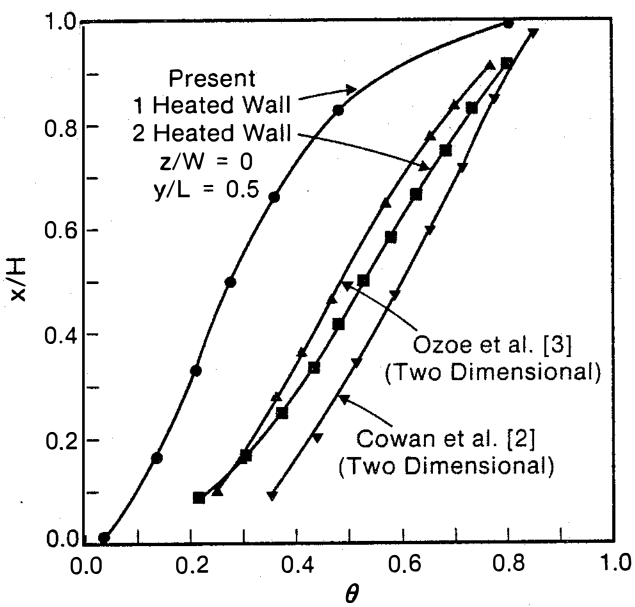

Figure 4. Temperature Distribution for z/W = 0, y/L = 0.5

Since the temperature profile in Figure 4 is typical of the entire core, the average core temperature θ_b may be calculated from

$$\int_0^1 \theta(x/H)d(x/H) \qquad (7)$$

Using the seven measurements of θ in Figure 4 and using the trapezoidal rule for integration, we find

$$\theta_b = 0.303 \cdot \qquad (8)$$

From equation (6) for $N_{HW} = 1$ we have

$$T_b = (T_h + 3T_c)/4 \; . \qquad (9)$$

Inserting equation (9) into equation (3) we find $\theta(T_b) = 0.25$, which compares favorably with 0.303. Repeating this procedure for the geometry with two heated walls we find an average, $\theta(T_b) = 0.44$ whereas using the average of the four wall temperatures gives $\theta_b = 0.50$ again reasonably close. In [1], we argued that the difference in temperature between the isothermal wall and the bulk flow temperature is the driving force for the flow in the boundary layer and hence heat transfer. This was confirmed by the heat transfer data. We have shown here that the choice of bulk fluid temperature, equation (6) used in [1] also compares favorably with the actual measured value.

Boundary layer temperature profiles are shown in Figure 5. All the profiles exhibit a large temperature gradient near the wall, reach a minimum near y = 2.8 mm, and increase slightly to asymptote to the core temperature for that height x at a distance from the heated wall of about 10 mm. The minimum temperature occurs only for enclosure flows and is apparently related to the interaction between the boundary layer and the stratified core fluid. It has been predicted numerically for air by Chen and Eichorn [4] and Newell and Schmidt [5] and has been seen experimentally by Eckert and Carlson [6] in air, by Elder [7] in oils by Ozoe et al. [3] in water as well as by several other researchers. Note that in the profiles θ (y = 0) < 1. This is the θ shift described in the previous section due to the finite probe size. Core stratification is also evident in the vertical shift in asymptote for the four temperature profiles. A lack of three-dimensional effect is demonstrated in the similarity of profiles number 2 and 3 which were for the same height x, but z/W = 0.25 and 0.5 respectively.

It is most convenient to present the local heat flux in terms of the local Nusselt number from equation (5). Following Cowan et al. [2], the local Rayleigh number is

$$Ra_x = \frac{g\beta x^3 (T_h - T_{x,\infty})}{\nu^2} Pr \qquad (10)$$

where the fluid properties are to be evaluated at the mean film temperature at height x.

The local Nusselt number is plotted as a function of Ra_x in Figure 6. Boundary layer profiles were measured at x = 7.62, 11.43, 15.24, 19.05, and 22.86 cm from the test cell floor at z = 0 and z/W = 0.417 to produce data at the five values of Ra_x shown in the figure. The five locations closest to the wall were used to determine the temperature gradient as discussed previously. In order to be consistent with Cowan et al [2], fluid properties were evaluated at the mean temperature

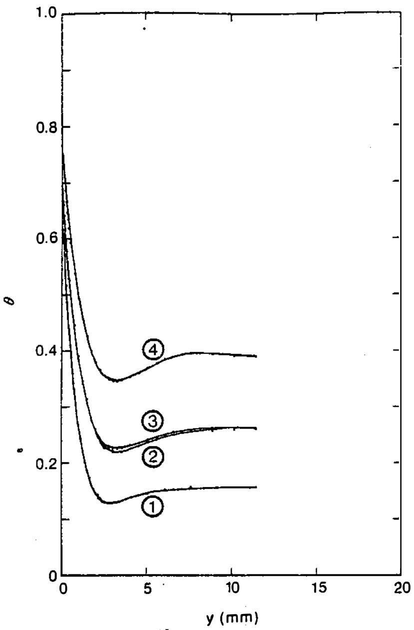

Figure 5. Boundary Layer Temperature Profiles 1: x/H = 0.25, z/W = 0; 2: x/H = 0.5, z/W = 0.25; 3: x/H = 0.5, z/W = 0; 4: x/H = 0.75, z/W = 0

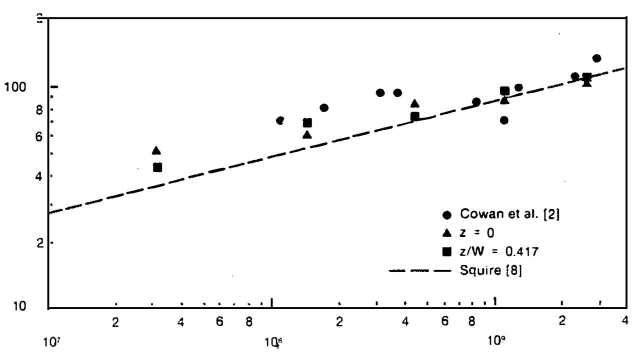

Figure 6. Local Heat Flux

in the boundary layer at the appropriate height x in the test cell.

There did not appear to be a large difference in Nu_z for the two values of z; however, for z/W = 0.417 the two highest Ra_z exhibited relatively large fluctuations in temperature implying turbulence. Also shown in the figure is the experimental data of Cowan [2] for a two-dimensional water filled enclosure and the analytical solution of Squire [8].

The present data bisects the Cowan data and compares favorably with Squire's analysis except at low Ra_z where the present data appears high. Also, the present data appear to fall better on a straight line than does Cowan's data but the slope of that line would be less than 0.25 predicted by Squire.

The foregoing implies that the local heat transfer is very much like that found in a two-dimensional geometry with the possible exception of unsteadiness near the upper cooled side walls in the present case. This similarity between the strongly three-dimensional geometry and two-dimensional geometry agrees with results of [1].

CONCLUSIONS

Detailed core temperature measurements in enclosures at high Rayleigh numbers show that, similar to two-dimensional enclosures, a three-dimensional enclosure exhibits core stratification. Temperature in the core varies only in the vertical direction even when the geometry and thermal boundary conditions are strongly three-dimensional, as in the present work. The distribution of core temperature is influenced by boundary conditions in a rather simple way. The distribution adjusts itself so that the average core temperature is approximately equal to the average of the four wall temperatures. For the geometry tested with one heated wall and three cooled walls, the isotherms are shifted up relative to the two-dimensional case, or the three-dimensional case with equal heated and cooled areas, giving a lower average core temperature. In the geometry tested with the two heated and two cooled walls, the temperature profile is close to previously published two-dimensional distributions.

Local heat flux measurements are in close agreement with two-dimensional enclosure data but exhibit a slightly weaker dependence upon local Rayleigh number than predicted by analyses. That is, the local Nusselt number versus local Rayleigh number plot exhibits a slope slightly less than the 1/4 slope predicted by laminar boundary layer theory.

These results are to be expected since the boundary layers at the high Rayleigh numbers in this study are thin. This implies that the influence of the boundaries, especially the corners, is only felt in a very small part of the enclosure flow. From the standpoint of building interiors, it appears that local as well as overall heat transfer rates may be estimated reasonably well from two-dimensional enclosure data. However, room temperature stratification is strongly dependent on boundary conditions and, therefore, cannot be determined from two-dimensional studies.

REFERENCES

1. Bohn, M. S., A. T. Kirkpatrick, D. A. Olson, "Experimental Study of Three Dimensional Natural Convection at High Rayleigh Number," J. Heat Transfer, Vol. 106, 1984, pp. 339-345.

2. Cowan, G. H., P.C. Lovegrove, and G. L. Quarini, "Turbulent Natural Convection Heat Transfer in Vertical Single Water-Filled Cavities," Proc. 7th Int. Heat Transf. Conf., Munich, Vol. 2, Hemisphere, Washington, D.C., 1982, pp. 195-203.